Korean J. Chem. Eng., **30**(5), 1076-1082 (2013)
DOI: 10.1007/s11814-013-0017-8

Bench-scale batch bioleaching of spent petroleum catalyst using mesophilic iron and sulfur oxidizing acidophiles

Haragobinda Srichandan*,, Dong-Jin Kim*, Chandra Sekhar Gahan*,***,†, Sradhanjali Singh*, and Seoung-Won Lee****

*Mineral Resource Research Division, Korea Institute of Geoscience and Mineral Resources (KIGAM), Gwahang-no 124, Yuseong-gu, Daejeon 305-350, Korea
**Nano Engineering Division, School of Engineering, Chungnam National University, Daejeon 305-764, Korea
***SRM Research Institute, SRM University, Kattankulathur - 603 203, Kancheepuram District, Chennai, Tamil Nadu, India
(*Received 30 September 2012 • accepted 6 February 2013*)

Abstract−Microbial leaching of a petroleum spent catalyst was carried out using mixed mesophilic iron and sulfur oxidizing acidophiles. Bench-scale batch stirred tank reactors with a working volume of 1 L were used in this study at 35 °C. The pulp density considered for the study was 10% (w/v), while the particle size of the spent catalyst was varied by 45-106, 106-212 and >212 μm. The leaching percentage of Ni from the spent catalyst was found to be highest (97-98%) with varying particle size. However, the leaching yield for rest of the metals like Al, Fe, V and Mo was 70-74%, 66-85%, 33-43% and 22-45%, respectively. Influence of particle size was predominant on the recovery of all metals except Ni. Assessment of the generation of the bioleach residue after bioleaching showed a weight loss of 54-62% due to the dissolution of the metal values from the spent catalyst. The mineralogical study conducted by X-ray diffraction and scanning electron microscopy supports the dissolution of metals from the spent catalyst. Jarosite mineral phase was the dominant mineral phase in the bioleach residue due to the dissolution of the oxidic and sulfidic mineral phases present in the feed spent catalyst.

Key words: Bioleaching, Microorganisms, Spent Catalyst, Population Dynamics, Redox Potential

INTRODUCTION

Depletion of primary metal resources in the earth's crust due to extensive mining has shifted the focus of mining and metal industries to utilizing secondary metal resources. The use of secondary metal resources would recycle waste byproducts rich in metal, helping to meet the current market demand for metals in a more efficient and cost effective manner. At present, the demand for metals is increasing due to the requirements for metals arising from economically and commercially developing nations like China, India and Brazil. The increasing demand, together with the huge tonnage of secondary resources as industrial wastes and urban wastes research in metallurgy, has naturally shifted towards the investigation of additional recycling. Among the existing types of secondary metal resources, spent hydroprocessing catalyst from oil refineries represents a waste rich in metals such as Al, Ni, Mo, V, Fe, Co etc. The annual production of petroleum refinery spent catalyst is approximately 150,000-170,000 tons/annum [1].

Petroleum refineries use huge amounts of solid catalysts for preparation of high grade fuel products from crude oil. During the refining process hydrotreated sulfur-containing gas-oil streams are transformed to low sulfur containing clean diesel fuels in the presence of catalysts. These catalysts consist of Mo and Co or Mo and Ni on porous γ-alumina support [2]. The metals present in the catalyst are both in the form of oxides and sulfides. During refining, the catalysts become deactivated over time and are regenerated for further use. Eventually, however, catalysts lose their ability to be reused and are finally discarded [3]. These waste spent catalysts have been classified as hazardous wastes by the United States-Environmental Protection Agency (US-EPA).

Several studies on hydrometallurgical routes for the recycling of spent catalyst have been carried out, with few of them being further developed to full-scale. Pyro-metallurgical processes, based on the principle of roasting and smelting of spent catalyst, require high inputs of energy [4,5].

As the pyro-process is energy intensive and requires a sophisticated gas cleaning system to prevent atmospheric pollution, hydrometallurgical processes based on acid and alkali leaching have been found to be advantageous. However, chemicals like strong acids and strong alkalis are not environmentally friendly and are hazardous in industrial applications. Some investigations have been carried out using strong acids, but the problem of such techniques lies in the composition of the inner lining of the tank to resist corrosion from strong acids or alkalis [6]. Several authors have reported the use of organic acid, or weak acids like oxalic acid together with hydrogen peroxide as an oxidant during the leaching of spent catalyst material. Similarly, others have used alkalis like sodium hydroxide for the leaching of spent catalyst [7-9]. Utilization of strong acid requires a large amount of basic material like lime or limestone to neutralize the acid downstream.

Recent advances in biohydrometallurgical research have revealed routes for bioleaching of chalcopyrite in both heap and stirred-tank reactors. Commercial advancement in this regards requires the micro-

†To whom correspondence should be addressed.
E-mail: chandrasekhar.g@res.srmuniv.ac.in, gahancsbiometal@gmail.com

biologist to work cooperatively together with the practitioners of the technology to develop mutual understanding of operational limitations and feasibility constraints affecting the process dynamics both in engineering and microbial aspects [10]. Ehrlich [11] reported the establishment of the rationale for the microbial mediated extraction of metal values from ores and concentrates. He also stated that there is a potential interaction of the microbes with the ores for microbial mediated ore beneficiation by bioleaching of unwanted metals or material from the ores keeping the metal of interest intact. Biohydrometallurgy could be a potential alternative process to pyrometallurgical and hydrometallurgical processes for the recovery of metal values from metal sulfides/oxides as well as industrial wastes [12-14]. Several research works have been carried out on bioleaching steel slag, lithium batteries, fly ash, spent batteries, electronic scrap materials and spent catalyst material [15-20]. Bioleaching of spent catalyst material on shake flask studies with a working volume of 100 ml at a pulp density 1-4% using both autotrophic and heterotrophic microorganisms resulted in a good recovery of metals. Bioleaching by using fungus and heterotrophic bacteria is always a challenge when it comes to scaling up the process, as it is difficult to maintain the closed and sterile systems required for each operation, which adds significant expense to such procedures [21-29]. The present study aimed to scale up the bioleaching of spent catalyst from shake flask studies conducted by previous authors, and investigate the metal recovery with three different sized fractions.

MATERIAL AND METHODS

1. Spent Catalyst

The spent catalyst material was received in bulk from a petroleum refinery of South Korea (SK Corporation). The spent catalyst sample received had an oily and black material sticking to its surface. The spent catalyst was pre-cleaned by acetone washing in a Soxhlet apparatus for 2-3 days to remove the organic deposits from the surface. The cleaned spent catalysts were then dried in a hot air oven at 50 °C until no change in weight was observed. The clean and dry spent catalysts were ground by mortar and pestle and were sieved to three different size fractions (45-106 μm, 106-212 μm and >212 μm). The elemental compositions of selected elements were determined by inductively coupled plasma - atomic emission spectroscopy (ICP-AES) for all three size fractions (Table 1). The mineralogy of the spent catalyst material was determined by X-ray diffraction (XRD) (Fig. 1) and scanning electron microscopy (SEM) using energy dispersive x-ray analysis (EDX) (Fig. 2).

Table 1. Chemical composition of selected elements in spent catalyst at different size fractions

Size fraction	Elemental composition (%)					
	S	Fe	Mo	V	Ni	Al
45-106	4.39	1.78	2.15	9.74	3.02	16.1
106-212	4.79	0.87	2.16	10.4	2.85	17.7
>212	5.3	0.64	1.93	13.5	3.03	16.6

2. Microorganisms and Growth Conditions

The microbial culture used for the bioleaching of spent catalyst material was a mixed culture of chemolithotrophic mesophilic acidophiles obtained from Lulea University of Technology, Lulea, Sweden. The culture was dominated by *Leptospirillum ferriphilum* (Fe-oxidizer) followed by *Acidithiobacillus caldus* (S-oxidiser), and

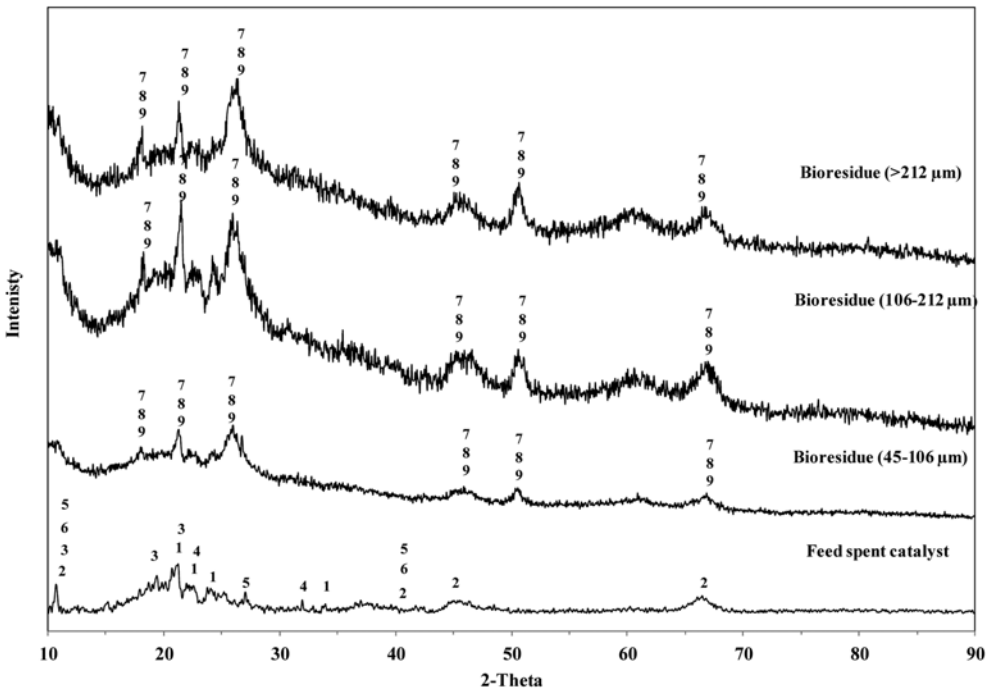

Fig. 1. XRD diffractogram of feed and bioresidue.

1. Molybndeum oxide (MoO_3)
2. Iron molybdenum sulphide ($Fe_{0.66}Mo_3S_4$)
3. Aluminum oxide (Al_2O_3)
4. Vanadium oxide (V_4O_9)
5. Nickel sulphide ($Ni_{3-x}S_2$)
6. Vanadium sulphide (VS_2)
7. Hydronium jarosites ($Fe_3(SO_4)_2(OH)_6$)
8. Sodium jarosite ($NaFe_3(SO_4)_2(OH)_6$)
9. Potassium jarosite ($KFe_3(SO_4)_2(OH)_6$)

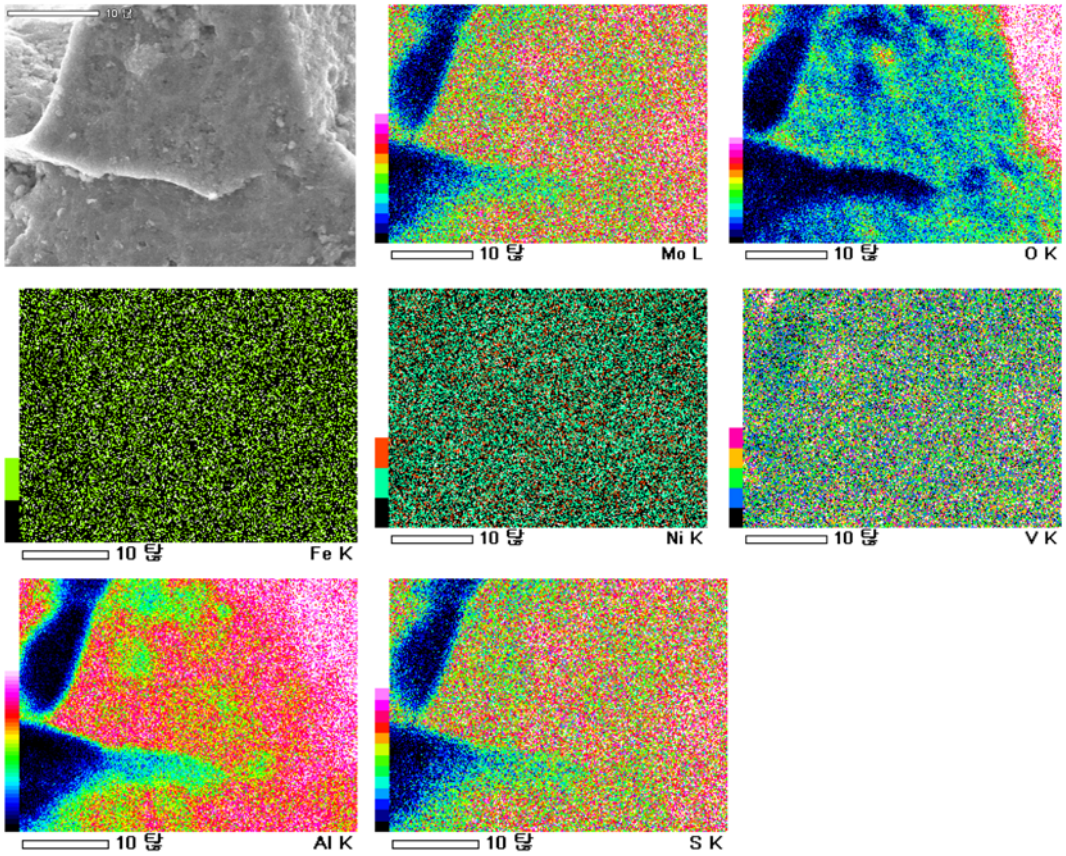

Fig. 2. SEM micrograph of feed spent catalyst with EDX analysis.

with approximately the same amount of *Acidithiobacillus thiooxidans* (S-oxidiser), *Sulphobacillus* sp. (Fe-oxidiser) and *Ferroplasma* (Archaeal species, Fe-oxidiser), as determined by Q-PCR analysis conducted at Bioclear B.V., Netherlands. The microbial culture was grown in a batch bioreactor using 9 K nutrient growth medium ($(NH_4)_2SO_4$, 3.0 g/L; KCl, 0.1 g/L; K_2HPO_4, 0.5 g/L; $MgSO_4 \cdot 7H_2O$, 0.5 g/L; $Ca(NO_3)_2 \cdot 4H_2O$, 0.01 g/L) [30] supplemented with 4.5 g/L of ferrous iron and 2 mM of potassium tetrathionate prior to its use. The inoculum was grown at a pH of 1.45±0.05 and at a temperature of 35 °C.

3. Instruments and Analytical Technique

A platinum electrode with an Ag, AgCl reference electrode was used for the measurement of the redox potential and a Lange LDO™/sc100 instrument was used for dissolved oxygen measurement. A portable pH meter (Orion) was used for pH measurements. ICP-AES (JOBIN-YVON JY 38) was used for elemental analysis of the spent catalyst material, as well as for the bioleached spent catalyst residue and leach liquor. Mineralogical studies of both the spent catalyst and bioleached residues were analyzed by XRD (RIGAKU, R4-200), equipped with a continuous scanning device using Cu Kα radiation at 40 kV and 30 mA with a sample rotation of 30 rpm, and the corresponding crystalline phases were identified using a file - Joint Committee for Powder Diffraction Standards (JCPDS) - in the instrument. SEM (JEOL, JSM-6380LA) was used to analyze the mineralogy of spent catalyst material and bioleached residues using EDX. The planktonic viable cell count was performed on a phase contrast microscope (Olympus Model No BX51TF) with a 10X eyepiece and a 40X objective resolution on an improved Neubauer haemocytometer.

4. Bioleaching Experiments

Bench-scale batch bioleaching of spent catalyst material for the three different size fractions (45-106 μm, 106-212 μm and ≥212 μm) was carried out in a 2.5 L baffled glass reactor at a working volume of 1 L. The batch experiments were conducted with 10% (w/v) of the spent catalyst material in iron free 9 K mineral salt medium (900 ml), which was inoculated with 100 ml mixed microbial culture. Homogenous mixing of the pulp was achieved using a propeller stirrer at a rotation of 350 rpm. A temperature of 35 °C inside the bioreactor was maintained by placing a hot plate beneath the reactor. A dissolved oxygen (D.O.) level of 5 mg/L was maintained inside the reactor by blowing air at a flow rate of 1 L/min underneath the propeller. The bioleaching experiment was conducted with regular measurements of pH, redox potential and planktonic viable cell count. The pH value in the bioleaching pulp was maintained at 1.5 throughout the experiment, by additions of 2 M/5 M H_2SO_4. During the initial days of the experiments there was a rise in pH due to the acid consuming oxide minerals present in the spent catalyst material, which was adjusted by addition of 2 M/5 M H_2SO_4 into the bioleaching pulp. The leaching experiments continued until no change in the pH or redox potential was observed. Water loss during bioleaching due to evaporation was compensated for with fresh additions of deionized water on a regular basis. On completion of the experiment, the bioleaching pulp was harvested and filtered by vacuum filtration for solid-liquid separation. The filter cake obtained after

filtration was thoroughly washed by using a measured volume of deionized water (acidified with H_2SO_4 to pH 1.5) to avoid precipitation of metal ions inside the filter cake. The washed filter cake was dried in hot air oven at 50 °C until no change in weight was observed. Later, the dry bioleached residue was fine-ground with a mortar and pestle and was sent for analysis for elemental composition by ICP-AES, and mineralogical analysis by XRD and SEM. The elemental analysis obtained was used for the calculation of the leaching yield, accounting the weight of the feed and bioleached residue. The percentage of leaching yield for all experiments was calculated as per the formula below:

$$\text{Leaching Yield (\%)} = \{1 - [\text{Me(r)}/\text{Me(f)}]\} * 100$$

where, Me(r) is the elemental (Fe, S, Ni, Al, Mo, V) content in the bioleach residue and Me(f) is the elemental (Fe, S, Ni, Al, Mo, V) content in the feed spent catalyst.

RESULTS AND DISCUSSION

Bioleaching of spent catalyst material using mesophilic iron and sulfur oxidizers with three different size fractions revealed the influence of particle size on leaching yield. The pulp density of 10% (w/v) for all the experiments was chosen, as it has been well established that in the operation of stirred-tank reactors the quantity of solids (pulp density) that can be maintained in suspension is limited to 10% (w/v). However, pulp densities >10% (w/v) would have problems with both the physical and microbial issues as the slurry becomes very thick with an inefficient O_2 and CO_2 transfer important for the bioleaching as well as microbial growth. At increased pulp densities >10% (w/v) a physical damage of microbial cells by the shear force of the impellers has been observed [31]. It is worth mentioning here that although no ferrous iron source was provided in the growth medium, the ferric iron in the inoculum, being reduced to ferrous iron, was sufficient for the initial oxidation of sulfides. The ferrous iron generated due to the oxidation of sulfides in the spent catalyst was re-oxidized to ferric iron by the iron oxidizing microorganisms present in the inoculum, whereas the dissolution of oxides present in the spent catalyst was carried out by the acid added to control the pH at 1.5. The free sulfur species generated due to the oxidation of sulfides of the spent catalyst was further oxidized by the sulfur oxidizing microorganisms into sulfates. Several parameters like pH, amount of acid added, redox potential, microbial population, temperature, dissolved oxygen and metal concentration were studied at regular intervals during the complete course of bioleaching.

1. Influence on the pH During Bioleaching and Acid Consumed

All three bioleaching experiments were performed under pH controlled conditions, where the pH of the bioleaching pulp was maintained at 1.5 to provide optimum pH conditions for the microorganisms, and to avoid ferric iron precipitation, which is in fact the primary oxidant for sulfide minerals present in the spent catalyst. A comparatively higher amount of acid consumption was observed during the first 2-3 days of the experiments due to the acid consuming oxides present in the spent catalyst (Eq. (1)).

$$MeO + H_2SO_4 \rightarrow MeSO_4 + H_2O \quad (1)$$

Once the dissolution of the all free oxide minerals was complete, the acid consumption started to decrease. Some part of the acid requirement was fulfilled from the acid produced due to jarosite precipitation towards the end of the experiment (Eq. (2)) [32,33].

$$X^+ + 3Fe^{3+} + 2SO_4^{2-} + 6H_2O \rightarrow XFe_3(SO4)_2(OH)_6 + 6H^+ \quad (2)$$

Where, $X^+ = K^+$, Na^+, H_3O^+, NH_4^+ …..

Apart from the oxidic minerals, the sulfidic minerals present in the spent catalyst were oxidized by ferric iron in the inoculum, resulting in the generation of ferrous iron in the solution (Eq. (3)) [34].

$$MeS + 2Fe^{3+} + 1.5O_2 + H_2O \rightarrow Me^{2+} + 2Fe^{2+} + SO_4^{2-} + 2H^+ \quad (3)$$

The ferrous iron in the solution was further re-oxidized biologically by the iron-oxidizing microorganisms in the bioleaching pulp, adding ferric iron back into solution for further oxidation of the residual sulfide minerals until they were all oxidized. As the ferrous iron oxidation is an acid-consuming process, some of the acid consumed during the bioleaching process is accountable for iron oxidation (Eq. (4)) [33,35-39].

$$Fe^{2+} + 1/4O_2 + H^+ \rightarrow Fe^{3+} + ½\ H_2O \quad (4)$$

Later, the sulfur species ($S_2O_3^{2-}$ or S^0) released from sulfide mineral dissolution into solution is oxidized by the sulfur-oxidizing microorganisms, which is an acid producing process, compensating part of acid consumption during the bioleaching of spent catalyst material (Eq. (5)).

$$S_2O_3^{2-} + 8Fe^{3+} + 5H_2O \rightarrow 2SO_4^{2-} + 8Fe^{2+} + 10H^+ \quad (5)$$

The total amount of acid consumed was calculated in terms of kilograms of H_2SO_4 required per ton of spent catalyst. The highest amount of acid was consumed in experiments of the smallest size fraction 45-106 μm, with 842 kg/ton consumed. The amount of acid consumed for size fraction 106-212 μm and >212 μm was 810 and 749 kg/ton, respectively (Table 2). The reason for the highest acid requirement of the smallest size fraction could be due to elevated liberation of the acid-consuming oxidic minerals from the spent catalyst due

Table 2. Total amount of sulfuric acid consumed for each experiment

Size fraction	Conc. sulfuric acid (kg/ton)
45-106	842
106-212	810
>212	759

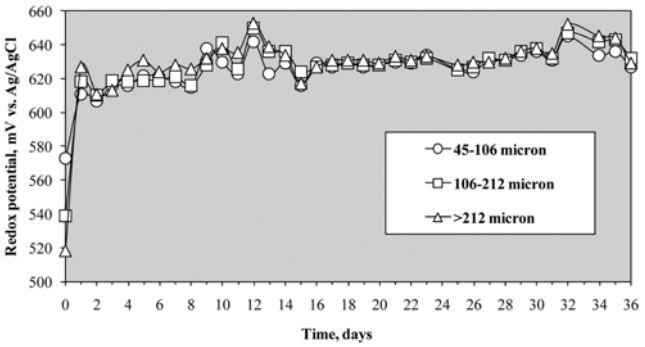

Fig. 3. Redox potential profile during the bioleaching of spent catalyst material.

to fine grinding.

2. Influence on the Redox Potential During Bioleaching of Spent Catalyst

The redox potential profile for all three size fractions presented in Fig. 3 states that the oxidation and reduction reactions occurred during the bioleaching of spent catalyst material. It was observed that the initial redox potential for all three size fractions was different, as 520, 540 and 575 mV for bioleaching experiments with size fractions >212, 106-212 and 45-106 μm, respectively (Fig. 3). This could be due to the faster dissolution of minerals in lower size fractions compared to higher ones. The higher dissolution of spent catalyst material at lower size fractions is in accordance with chemical leaching theory (chemically controlled and diffusion controlled reaction) [22]. From the leaching theories described above, it is evident that the rate of reaction is inversely proportional to the radius of the substrate particle in chemically controlled leaching, while the rate of reaction is inversely proportional to the square of the radius of the particle.

However, it is well known, and somewhat instinctive, that the smaller the size fraction the better the dissolution rate, as smaller size fractions provide more surface area compared to larger size fractions. The fast dissolution of the spent catalyst, starting from the initial days of the experiment until 12-14 days, increased the redox potential, which later started to drop, probably due to the precipitation of ferric iron as jarosite [33]. The redox potential value obtained due to the ferric/ferrous couple is always found to be dominant, but the influence on the redox potential value due to other redox couples present in the solution such as Mo, V, Ni and Al cannot be ignored. Overall, the redox potential stabilized between 600-640 mv towards the end of all experiments (Fig. 3).

3. Influence on the Planktonic Viable Microbial Population Dynamics

The microbial population dynamics during the bioleaching of spent catalyst was determined by planktonic viable cell count. The cell count was carried out to ensure the viable cell population's activity during the process of bioleaching, as well as to provide information on the influence of size fractions. Microbial population study shows that the viable planktonic cell count ranged between 10^6-10^7 cells/ml in the bioleaching pulp (Fig. 4). The planktonic viable cell population in three different size fractions did not show any remarkable difference, as no toxic influence was encountered due to the metal ions present in the spent catalyst. The results obtained from the microbial population dynamics indicate that these microorganisms can be sustained and can carry out bioleaching without any hindrance or toxic effect of the spent catalysts. There was no such difference in the cell count of the experiments with 45-106 μm and 106-212 μm size fractions. The microbial cell population increased from 3.5×10^5 to 8.2×10^6 cells/ml in the 45-106 μm size fraction experiment, and from 8.5×10^5 to 8.5×10^6 cells/ml in the 106-212 μm size fraction experiment; however, in the case of the >212 μm size fraction experiment the cell count was found to be highest among all. The reason for which could be due to a reduced toxic influence from metal ions due to the slightly lower dissolution kinetics. Overall, the population dynamics were satisfactory in all three experiments.

4. Bioleaching Yield with Different Size Fractions of Spent Catalyst

The bioleaching yield was calculated based on the chemical composition of the spent catalyst as feed (Table 1) and the chemical composition of the bioleached residue obtained (Table 3), considering the weight of the catalyst material assed to the experiment (Table 4). The bioleached residue obtained from the bioleaching experiments was found to have weight loss, due to the dissolution of the mineral phases, both by acid leaching and ferric iron mediated leaching. It has been found that the smallest size fraction encountered the highest

Table 3. Chemical composition of the selected elements in the bioleaching residue

Size fraction	Elemental composition (%)					
	S	Fe	Mo	V	Ni	Al
45-106	2.77	0.88	3.06	14.6	0.16	10.9
106-212	2.57	0.74	2.98	15.1	0.15	12.3
>212	2.60	0.80	3.26	19.5	0.18	10.1

Table 4. Change in weight of the feed and bioleaching residue

Size fraction (μm)	Wt of feed (g)	Wt of bioleaching residue (g)	% Loss in Wt
45-106	100	38	62%
106-212	100	43	57%
>212	100	46	54%

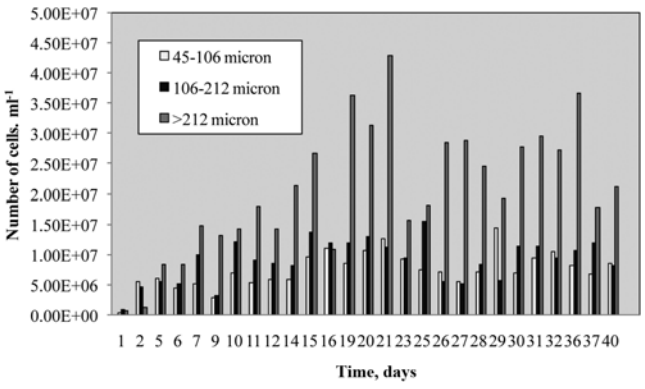

Fig. 4. Planktonic microbial population dynamics during the bioleaching of spent catalyst.

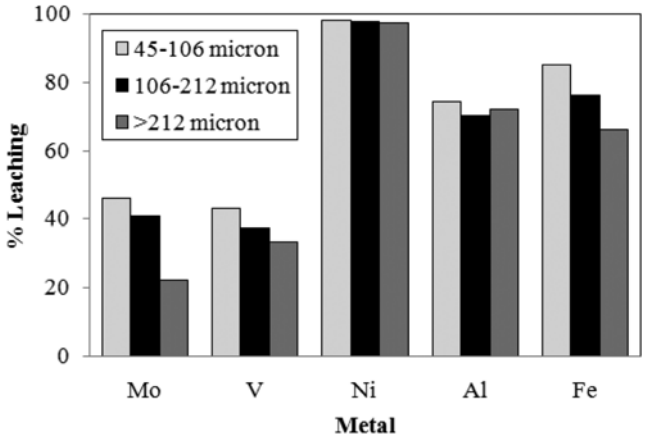

Fig. 5. Leaching yield of metal values with different size fractions.

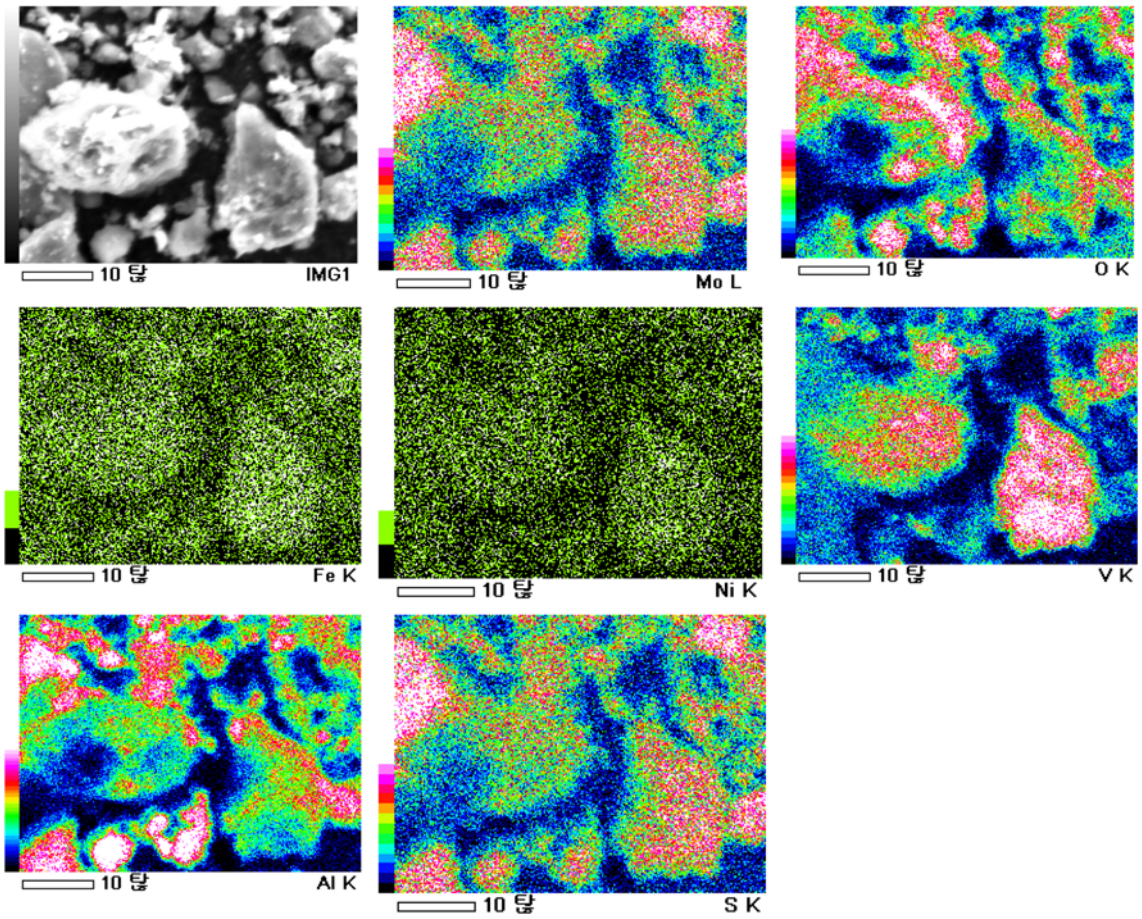

Fig. 6. SEM micrograph of bioleach residues with EDX analysis.

weight loss of 62%, followed by 57% and 54% for the higher size fractions, respectively, and was considered to be due to the higher dissolution rate with smaller size fractions as stated in Eqs. (6) and (7). The leaching yield for Ni was found to be invariable with all the three size fractions, with slightly small variation in the leaching yield of bigger size fractions (Fig. 5). However, the leaching yield of Mo, V and Fe has shown a remarkable decrease in the dissolution rate with increasing size fractions, whereas in the case of Al, the yield was found to be more or less similar with large and small sized fractions (Fig. 5).

Mineralogical analysis of the feed spent catalyst revealed the presence of oxide and sulfide mineral phases of Ni, V, Mo. Al and Fe (Fig. 1). After completion of the bioleaching experiment a significant amount of weight loss was observed in the bioleached residue, probably due to dissolution of the mineralogical phases present in the spent catalyst, and can be explained from the XRD analysis of the bioleach residues (Fig. 1). The major mineral phase observed in the bioleached residue was the hydronium/potassium/sodium jarosites, which were precipitated during the bioleaching process. The oxidic and sulfidic mineral phases present in the feed spent catalyst material were mostly absent in the bioleach residues (Figs. 1 and 6). The micrographs of the feed spent catalyst and bioleach residues obtained from scanning electron microscopy (SEM) support the XRD analysis. The EDX analysis of the SEM micrograph of feed spent catalyst shows the presence of Molybdenum, sulfur and oxygen complex, as Molybdenum sulfides and oxides together with Aluminum oxides (Fig. 1 and 6). Further mineralogy of nickel and vanadium oxides/sulfides observed in XRD analysis was not detected through SEM-EDX analysis of the feed spent catalyst sample. The bioleached residue showed fragmented pictures confirming the dissolution of the oxides/sulfides of Mo, V and Al compared to the feed material (Fig. 6). The unclear shape of the Ni-Fe oxides or sulfides region was also observed only in the bioleached residue. The dissolution of the Mo, V, Al and Fe observed from the leaching yield was incomplete, as can be seen from the weight loss and fragmented pictures from the EDX analysis of the SEM micrographs. Therefore, it can be assumed that some part of undissolved Mo, V and Al could be dissolved by further developing the bioleaching to a continuous stirred tank bioleaching with two- or three-stage leaching. Some passivation of the sulfur species on the spent catalyst might be obstructing the leachate from reaching the surface of the spent catalyst.

CONCLUSION

All the three size fractions of the spent catalyst studied for the bioleaching experiment showed an increasing trend of leaching yield for Mo, V and Fe, with decreasing size fractions, but in the case of Ni there was no remarkable difference in the leaching yield. The leaching yield of Ni was the highest among all other elements, ranging from 97-98%, which means nickel mineral present in spent cata-

lyst could be easily liberated via grinding. The mineralogical studies by XRD analysis indicated that the major mineralogical phases found in the feed spent catalyst were dissolved during bioleaching, and that the formation of new phases, like jarosites, occurred due to the precipitation of ferric iron. The micrographs of SEM analysis supported the mineral phases of sulfides and oxides observed by XRD analysis in the feed material. The fragmented pictures of those oxides and sulfides seen in the SEM micrograph after bioleaching confirm the incomplete dissolution of the minerals present in the feed material. The microbial population dynamics observed suggests that these mixed mesophilic microbes had luxuriant growth under the current bioleaching conditions. The bioleaching of spent catalyst material is partly carried out by acid mediated dissolution, and partly by ferric ion. The acid requirement is fulfilled by sulfur oxidation as well as external additions of H_2SO_4, whereas the ferric iron requirement is fulfilled by the oxidation of ferrous iron by the iron oxidizing microorganisms. Bioleaching of spent catalyst material in batch bioreactor with optimum growth conditions has been found to be promising for larger scale experiments in a continuously stirred tank bioreactor. However, this study shows the possibility of bioleaching of spent catalyst at elevated pulp densities only if carried out in 2-3 stage continuous reactors. This would enhance reaction kinetics and help to obtain better or similar yields of metal values at a shorter retention times. Use of cost-effective iron-free 9 K growth medium for the microbial growth would also lead to an overall supplement to the process economics. Future studies should mostly focus on enhancing the Mo and V recovery by liberating the mineral from the matrix of spent catalyst, which could be done by employing either metallurgical process or biological mediated process considering the environmental and economic issues.

ACKNOWLEDGEMENT

This research was supported by Leading Foreign Research Institute Recruitment Program through the National Research Foundation of Korea (NRF) funded by the Ministry of Education, Science and Technology (MEST) (2011-00123). The authors would like to thank Prof. Åke Sandström, Lulea University of Technology, Sweden for providing the microbial culture used in the present study.

REFERENCES

1. M. Marafi and A. Stanislaus, *Resour. Conserv. Recycl.*, **52**, 859 (2008).
2. C. Song, *Catal. Today*, **86**, 211 (2003).
3. D. L. Trimm, *Appl. Catal. A: Gen.*, **212**, 153 (2001).
4. G. Parkinson and S. Isho, *Chem. Eng.*, **94**, 25 (1987).
5. R. G. Busnardo, N. G. Busnardo, G. N. Salvato and J. C. Afonso, *J. Hazard. Mater.*, **139**, 391 (2007).
6. S. P. Barik, K. H. Park, P. K. Parhi and J. T. Park, *Hydrometallurgy*, **111-112**, 46 (2012).
7. A. Szymczycha-Madeja, *J. Hazard. Mater.*, **186**, 2157 (2011).
8. E. A. Abdel-Aal and M. M. Rashad, *Hydrometallurgy*, **74**, 189 (2004).
9. A. Ognyanova, A. T. Ozturk, I. De Michelis, F. Ferella, G. Taglieri, A. Akcil and F. Vegliò, *Hydrometallurgy*, **100**, 20 (2009).
10. J. A. Brierley and C. L. Brierley, *Hydrometallurgy*, **59**, 233 (2001).
11. H. L. Ehrlich, *Euro. J. Min. Proc. Environ. Protect.*, **4**, 102 (2004).
12. S. Panda, C. K. Sarangi, N. Pradhan, T. Subbaiah, L. B. Sukla, B. K. Mishra, G. L. Bhatoa, M. Prasad and S. K. Ray, *Korean J. Chem. Eng.*, **29**, 781 (2012).
13. C. S. Gahan, D. J. Kim, H. Srichandan and A. Akcil, *Res. J. Recent Sci.*, **1**, 85 (2012).
14. S. Panda, K. Sanjay, L. B. Sukla, N. Pradhan, T. Subbaiah, B. K. Mishra, M. S. R. Prasad and S. K. Ray, *Hydrometallurgy*, **125-126**, 157 (2012).
15. C. S. Gahan, M. L. Cunha and Å. Sandström, *Hydrometallurgy*, **95**, 190 (2009).
16. C. S. Gahan, J. E. Sundkvist and Å. Sandström, *Miner. Eng.*, **23**, 731 (2010).
17. D. Mishra, D. J. Kim, D. E. Ralph, J. G. Ahn and Y. H. Rhee, *Waste Manage.*, **28**, 333 (2008).
18. B. Xin, D. Zhang, X. Zhang, Y. Xia, F. Wu, S. Chen and L. Li, *Bioresour. Technol.*, **100**, 6163 (2009).
19. W. Burgstaller and F. Schinner, *J. Biotechnol.*, **27**, 91 (1993).
20. P. P. Bosshard, R. Bachofen and H. Brandl, *Environ. Sci. Technol.*, **30**, 3066 (1996).
21. C. Cerruti, G. Curutchet and E. Donati, *J. Biotechnol.*, **62**, 209 (1998).
22. D. Pradhan, D. J. Kim, J. G. Ahn, C. S. Gahan, H. S. Chung and S. W. Lee, *Korean J. Met. Mater.*, **49**, 956 (2011).
23. L. A. Mutch, H. R. Watling and E. L. J. Watkin, *Hydrometallurgy*, **104**, 391 (2010).
24. D. Mishra, J. G. Ahn, D. J. Kim, G. Roychaudhury and D. E. Ralph, *J. Hazard. Mater.*, **167**, 1231 (2009).
25. D. Mishra, D. J. Kim, D. E. Ralph, J. G. Ahn and Y. H. Rhee, *Hydrometallurgy*, **88**, 202 (2007).
26. V. Bosio, M. Viera and E. Donati, *J. Hazard. Mater.*, **154**, 804 (2008).
27. F. Beolchini, V. Fonti, F. Ferella and F. Veglio, *J. Hazard. Mater.*, **178**, 529 (2010).
28. R. M. Gholami, S. M. Borghei and S. M. Mousavi, *Hydrometallurgy*, **106**, 26 (2011).
29. D. Pradhan, D. Mishra, D. J. Kim, J. G. Ahn, G. R. Chaudhury and S. W. Lee, *J. Hazard. Mater.*, **175**, 267 (2010).
30. M. P. Silverman and D. G. Lundgren, *J. Bacteriol.*, **77**, 642 (1959).
31. D. E. Rawlings, D. Dew and C. D. Plessis, *Trends. Biotechnol*., **21**, 38 (2003).
32. J. E. Dutrizac, *Metall. Trans. B*, **14**, 531 (1983).
33. C. S. Gahan, J. E. Sundkvist and Å. Sandström, *J. Hazard. Mater.*, **172**, 1273 (2009).
34. A. Akcil and H. Deveci, *Geomicrobiology*, Science Publishers, New Hampshire, USA (ISBN: 978-1-57808-665-8), 101 (2010).
35. A. Schippers and W. Sand, *Appl. Environ. Microbiol.*, **65**, 319 (1999).
36. H. Tributsch, *Hydrometallurgy*, **59**, 177 (2001).
37. W. Sand, T. Gehrke, P. G. Jozsa and A. Schippers, *Hydrometallurgy*, **59**, 159 (2001).
38. T. Rohwerder, T. Gehrke, K. Kinzler and W. Sand, *Appl. Microbiol. Biotechnol.*, **63**, 239 (2003).
39. D. E. Rawlings, D. Dew and C. D. Plessis, *Trends Biotechnol.*, **21**, 38 (2003).